Tuning Interlayer Exchange Coupling of Co-Doped TiO_2/VO_2 Multilayers via Metal-Insulator Transition

Z. Tang,* F. Sun, B. Han, K. Yu, Z. Q. Zhu, and J. H. Chu

Key Laboratory of Polar Materials and Devices, Ministry of Education, East China Normal University, Shanghai 200241, People's Republic of China

(Received 24 July 2013; published 4 September 2013)

Reversibly switching interlayer exchange coupling (IEC) of magnetic semiconductor multilayers between ferromagnetic (FM) and antiferromagnetic (AFM) modes is a difficult but key issue for fabricating semiconductor giant magnetoresistance devices. Here, we show that such tunable IEC is achievable around room temperature in Co-doped TiO_2/VO_2 diluted magnetic semiconductor multilayers. On the basis of first-principles calculations of electronic structure and fermiology, it is clarified that, associated with the metal-insulator transition (MIT) of nanosized VO_2 spacers, exotic short-range magnetic orders are developed in the multilayers so that the IEC can be tuned reversibly from FM mode to AFM mode by varying temperature crossing the MIT (~ 340 K).

DOI: 10.1103/PhysRevLett.111.107203 PACS numbers: 75.50.Pp, 71.30.+h, 75.70.Cn, 85.75.−d

Interlayer exchange coupling (IEC) plays an important role in manipulating transport properties of magnetic multilayers because the spin-dependent carrier scattering can be changed greatly by switching the IEC between ferromagnetic (FM) and antiferromagnetic (AFM) modes. The IEC has demonstrated its technological impact in the form of metallic giant magnetoresistance (GMR) effect and has initiated the emergence of spintronics [1,2]. There has been great interest in magnetic semiconductor multilayers [3–12], as they can assure the integrability of novel spintronics with well-established semiconductor technology. However, after intensive studies since the late 1980s [3], one has realized that switching the IEC of semiconductor multilayers is rather difficult. Although the AFM IEC and the oscillatory IEC have been predicted based on the general Ruderman-Kittle-Kasuya-Yosida (RKKY) theory [10–12], experimental observations have mostly shown the FM IEC [3–5]. Only very recently, direct evidence of the AFM IEC was reported in (MnGa)As/GaAs:Be diluted magnetic semiconductor (DMS) multilayers [6–8].

In this Letter, we argue that although the FM IEC of the semiconductor multilayers is an intrinsic characteristic associated with the band gap, the reversibly tunable IEC is achievable at around *room temperature* in Co-doped TiO_2/VO_2 DMS multilayers via metal-insulator transition (MIT). Here, the Co-doped rutile TiO_2, a well-studied DMS material of room-temperature ferromagnetism [13,14], was employed for the magnetic layers. VO_2 was chosen for the spacers, which undergoes a MIT at 340 K accompanied by a structural transition from the semiconducting monoclinic ($M1$) phase to the high-temperature conducting rutile (R) phase [15]. As the lattice mismatch between the rutile TiO_2 ($a = 4.593$ Å and $c = 2.959$ Å) and VO_2 (4.555 and 2.851 Å) [16] is very small, their heterostructures and interfaces have received extensive attention and interesting properties have been explored [17,18]. On the basis of first-principles calculations, we show that the IEC of the Co-doped TiO_2 DMS layers can be reversibly switched between FM and AFM modes by varying the temperature crossing the MIT. Such an exotic characteristic can be utilized to fabricate DMS-based GMR devices operating at around room temperature.

The DMS multilayers were simulated by using slab supercells. As illustrated in Fig. 1, the supercell of each model DMS multilayer consists of two rutile TiO_2 layers (with a fixed thickness of $m = 4$ slabs) separated by a VO_2 spacer (n slabs). The Ti atoms near two interfaces in the model multilayer were substituted by Co atoms so that two Co-doped TiO_2 DMS layers were obtained. An R-phase VO_2 spacer of thickness n was trivially constructed by stacking n building blocks of $1 \times 2 \times 1$ rutile VO_2 unit cells along the c axis. An $M1$-phase VO_2 spacer of thickness n (Fig. 1) was obtained by dimerizing and distorting the V–V pairs along the c axis in the corresponding R-phase spacer [19].

It is well-known that a Peierls-like phase transition results from the pairing distortion of atoms in the neighboring unit cells so that the unit cell doubles after the phase transition. For VO_2, it is noticed that in addition to the pairing along the c axis, the twisting of the V ions after the MIT is actually equivalent to another pairing of the V ions along the prolonged V–O bond direction (the distorted octahedron of the rutile VO_2 has four shorter V–O bonds of 1.92 Å and two longer V–O bonds of 1.93 Å). Therefore, the $M1$-phase VO_2 spacer can be obtained as shown in Fig. 1. Particularly, the large orthogonal unit cell shown in Fig. 1, obtained by doubling the rutile unit cell along the b and c axes, is common for both the R- and $M1$-phase VO_2, indicating that the well-matched epitaxial structures of the multilayers are maintained after the MIT.

Our first-principles calculations were performed by using the L(S)DA + U scheme implanted in the

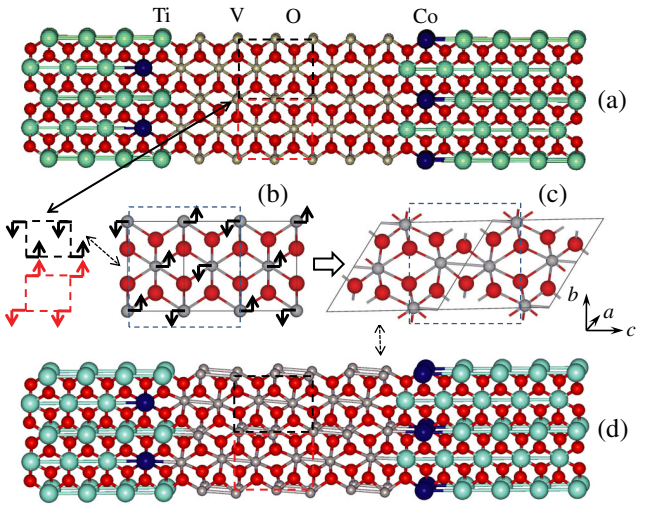

FIG. 1 (color online). Structure of Co-doped TiO_2/VO_2 multilayers and their variations in metal-insulator phase transition. Top (a): the multilayer with an R-phase VO_2 spacer. The combination of two building blocks of the rutile VO_2 layer (black and red rectangles) forms a large orthogonal unit cell matching well the Co-doped TiO_2 layers. Middle [(b) and (c)]: distorting the atoms in the building blocks of the R-phase VO_2 spacer following the arrows (b) results in the monoclinic unit cells of the $M1$-phase VO_2 (c). Bottom (d): the multilayer with the $M1$-phase VO_2 spacer.

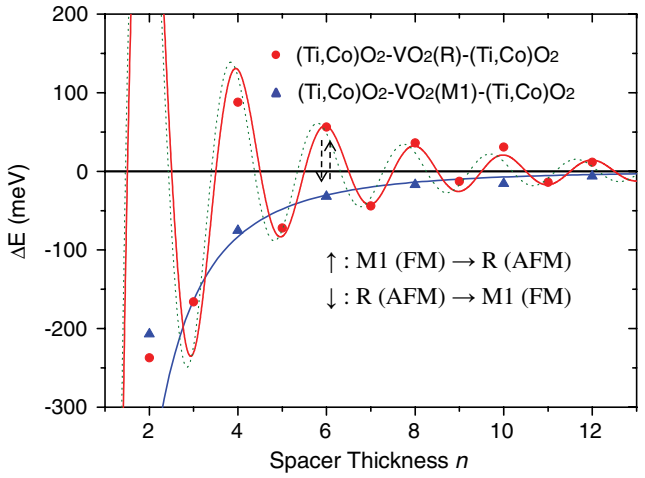

FIG. 2 (color online). Calculated IEC as a function of the spacer thickness, and circles and triangles denote the calculated results for the R-phase and the $M1$-phase VO_2 spacers, respectively. Solid (dashed) line denotes the theory-predicted oscillatory function with a period of $\lambda = 2c$ ($1.94c$). Vertical arrows denote that increasing or decreasing temperature crossing the phase-transition point can reversibly switch the IEC between ferromagnetic and antiferromagnetic.

QUANTUM-ESPRESSO package [20]. Details about the calculations can be found in the Supplemental Material [21]. By careful tweaking of the pseudopotentials and the on-site Hubbard parameters U and J, the calculations well reproduce the band structures of bulk VO_2 in both the R and $M1$ phases: as shown in Fig. S1 of the Supplemental Material [21], a semiconductor band structure is obtained for the $M1$ phase and the calculated band gap is 0.25 eV, about half of the experimental value (~ 0.6 eV) [15]. We focus on the perpendicular magnetization of the DMS multilayers, i.e., the magnetization directions aligned either parallel (FM ordering) or antiparallel (AFM ordering) to the c axis. The total energies of these two magnetic configurations were calculated, and the IEC was obtained as the energy difference, $\Delta E = E_{\mathrm{FM}} - E_{\mathrm{AFM}}$.

In the present model multilayers, three kinds of magnetic interactions may contribute to the calculated ΔE, namely, indirect IEC ΔE_1 and ΔE_2 through the middle VO_2 spacer and through the side TiO_2 layers, respectively, and a possible direct magnetic interaction between the DMS layers (which is negligible when the spacer is thick enough). By replacement of the middle VO_2 spacer by an undoped TiO_2 layer with different thickness, ΔE_2 of the present model multilayers is estimated to be only about 3.0 meV and thereby is negligible (Supplemental Material [21]). Figure 2 presents the calculated IEC through the $M1$-phase VO_2 spacer as a function of thickness n. It is observed that, for all the calculated $M1$-phase VO_2 spacers, the FM configuration of the two DMS layers is always energetically favorable (i.e., $\Delta E < 0$) and from $n = 2$ to 12 $|\Delta E|$ rapidly decreases from 207.1 to 6.3 meV. As a matter of fact, a similar monotonic decrease in $|\Delta E|$ with increasing n is also observed when the $M1$-phase VO_2 spacers are replaced by the undoped TiO_2 spacers (Fig. S2 of the Supplemental Material [21]), indicating that it is common for the semiconducting spacers.

The conventional RKKY theory predicts a FM-AFM oscillatory IEC with increasing the spacer thickness in metallic multilayers. Nevertheless, on the basis of a two-band model Abrikosov [22] and Narita and Kasuya [23,24] studied the RKKY interaction mediated by valence-conduction band excitations in intrinsic semiconductors in the 1980s and later Litvinov and Dugaev [25] studied the one originated from impurity-valence band excitations in Mn-doped GaAs. It has been shown that because of the imperfect spin screening effect the indirect RKKY interaction in gapped systems is ferromagnetic and its amplitude decays exponentially as $J(R) \propto e^{-\beta R}/R^2$ in the two dimensions [26,27], where $\beta = 2\sqrt{m^* E_g}$ is an exponential decay prefactor depending on the effective mass of the carriers (m^*) and on the energy gap (E_g) and $R = nc$ is the distance between the magnetic layers. Taking β as a fitting parameter, we obtain the thickness-dependent IEC as ΔE (eV) $= -1.344e^{-0.301n}/n^2$ and ΔE (eV) $= -2.010e^{-0.102n}/n^2$ for the TiO_2 and $M1$-phase VO_2 spacers, respectively. As shown in Fig. S2 of the Supplemental Material [21], these model functions indeed describe reasonably the trends of ΔE. As the calculated band gap of the $M1$-phase VO_2 (0.25 eV) is smaller than

that of TiO_2 (2.41 eV), a slower decay in ΔE is expected for the VO_2 spacers (Supplemental Material [21]).

So far, the calculations indicate that the ferromagnetic IEC of the semiconductor multilayers originates from the spacer's band gap so that if an intrinsic (or a low doped) semiconductor spacer is employed, only the ferromagnetic IEC can be obtained. To obtain an antiferromagnetic IEC, heavy doping in the spacer layers is necessary to produce "metalliclike" carrier bands to mediate the IEC, as supported by the recent theory [10,11,25–27] and experiment [6]. This mechanism reminds us that the MIT may be an alternative way even more effective to manipulate the IEC of the DMS multilayers. For this reason, we next study the IEC mediated by the metallic rutile VO_2 spacers.

It is found from the calculations that in the magnetic multilayer environment, the unpaired $3d^1$ electrons of V^{4+} in the rutile VO_2 not only make the spacer metallic [15,18] but also exhibit considerable magnetic response to the magnetic DMS layers, which in combination with the spin interaction among the V^{4+} ions leads to abundant features in the magnetic structures of the DMS multilayers. To demonstrate this, we compare in Fig. 3 the calculated spin-density distributions in the multilayers with $n = 5$ (odd) and 6 (even) with the two magnetic DMS layers in both the FM and AFM configurations.

Although the four spin-density distributions shown in Fig. 3 are different from each other, there are two important common characteristics: (1) around the interfaces, the local magnetic moments of the V ions tend to align parallel to those of the nearby magnetic DMS layers, indicating a ferromagnetic interaction between them, and (2) no matter what the interface magnetic structures are, the V ions in each one-dimensional (1D) chain along the c axis always couple antiferromagnetically. As a result, in the cases of the two DMS layers in the FM configuration, the magnetic orders of the whole multilayers are ⇑ (⇑⇑⇓ ... ⇓⇑⇑) ⇑ and ⇑ (↑⇓⇓↑ ... ↑⇓⇓↑) ⇑ for the spacer thickness n = odd and even, respectively (here ⇑ / ⇓ and ↑ / ↓ denote, respectively, the magnetic moments of the DMS layers and of the V ions). Whereas in the cases of the AFM configuration, the overall magnetic orders are either ⇓ (⇓⇑⇑ ... ↑⇓⇓↑) ⇑ (odd) or ⇓ (⇓⇓⇑⇑ ... ⇓⇓⇑⇑) ⇑ (even).

The calculated total energies show that, for n = odd (even), the FM (AFM) configuration of the two DMS layers has the lower energy, i.e., the magnetic structures having more ferromagnetically coupled layers around the interfaces are energetically favorable (⇑ (⇑⇑⇓ ... ⇓⇑⇑) ⇑ for n = odd and ⇓ (⇓⇓⇑⇑ ... ⇓⇓⇑⇑) ⇑ for n = even). As a result, when $n \geq 3$, the calculated ΔE oscillates between FM and AFM modes with an oscillatory period of $\lambda = 2c$ (Fig. 3). Furthermore, we performed a discrete Fourier transform for the calculated ΔE to resolve quantitatively the IEC period (Fig. S4 in the Supplemental Material [21]). A dominant peak at $q = 1.005\pi/c$ is observed, indicating that the calculated oscillatory period is $1.99c$. To explain

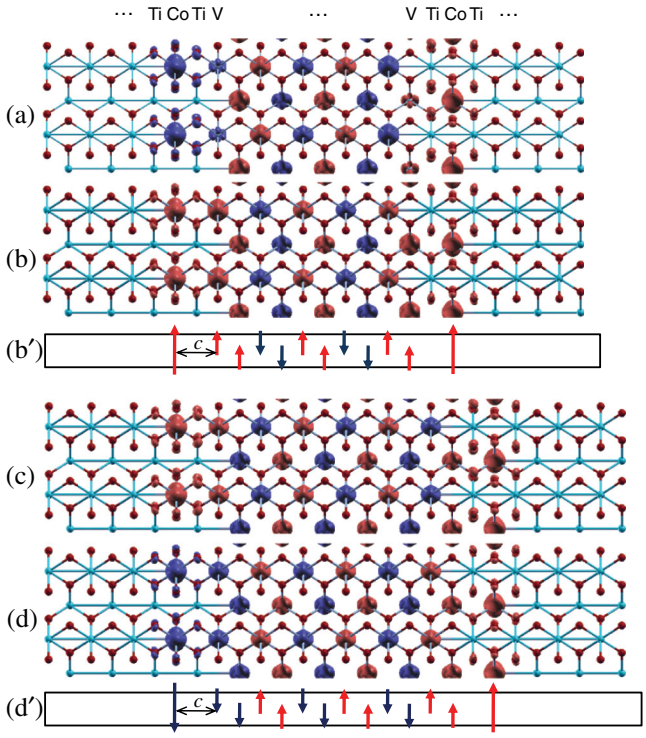

FIG. 3 (color online). Calculated spin-density distributions in the Co-doped TiO_2/VO_2 multilayers with the VO_2 spacer thickness $n = 5$ [(a) and (b)] and 6 [(c) and (d)]. In (a) and (d) [(b) and (c)], the two DMS layers are in the antiferromagnetic (ferromagnetic) configuration. (b) [(d)] is the ground state for $n = 5$ (6), and its magnetic structure is sketched in (b′) [(d′)].

the oscillatory IEC of metallic magnetic multilayers, Bruno and Chappert [28] have proposed an extended RKKY theory taking into account the spacer's fermiology. It has been shown that the oscillatory period is controlled by the singular wave vector $\mathbf{q}_s$, which links a pair of Kohn singularities on the spacer's Fermi surface (FS) along the orientation of the multilayers (or by the beat frequencies of $\mathbf{q}_s$'s). It is therefore interesting to see if the theory still holds in the DMS multilayers.

The calculated fermiology of the R-phase VO_2 (see Fig. S3 of the Supplemental Material [21]) shows that there are totally three bands crossing the Fermi level, but the third band contributes only a small portion, and its effect in mediating the IEC is thus omitted. As for the first and second bands, although their FS sheets are complicated, we notice that all of them can be reproduced by folding a simple Fermi surface. Figure 4 presents the cross sections of these multi-FS sheets on the [010] plane in the extended zone scheme. The shape of these cross sections agrees well with the previously reported results [15]. The jointed shadow area (i.e., the occupied momentum states) in the extended zone scheme shows clearly that the Fermi surface of the R-phase VO_2 is a corner-deformed, prolonged, hollow octahedron. Therefore, two singular wave vectors along the c axis are identified as $\mathbf{q}_1 = (0, 0, 1.03\pi/c)$ and

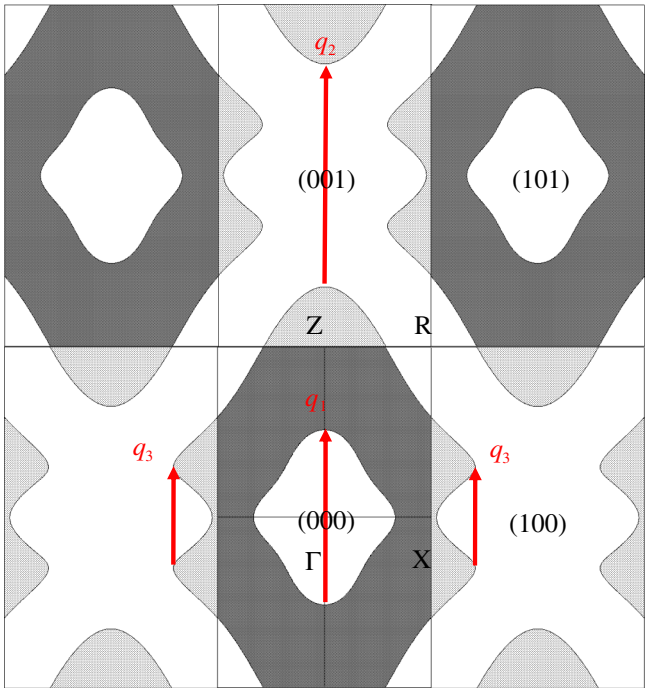

FIG. 4 (color online). Fermi surface cross sections of the rutile VO_2 bulk on the [010] plane (through the Γ point) in the extended zone scheme. Light and dark shadowed areas denote the occupied momentum states of the first and second bands, respectively.

$\mathbf{q}_2 = (0, 0, 1.32\pi/c)$ ($\mathbf{q}_2$ associated with a umklapp process), where any pair of k points on two small pieces of Fermi surface containing the Kohn singular points approximately satisfies the condition $\mathbf{k}_1 - \mathbf{k}_2 = \mathbf{q}_i$ ($i = 1$ or 2). There also may be other possible singular wave vectors, for instance, $\mathbf{q}_3 = (0, 0, 0.60\pi/c)$ connecting two "hilltops" k points in Fig. 4. However, in this case only few k states satisfy the above condition so that these singular vectors are less important.

The singular wave vectors $\mathbf{q}_1$ and $\mathbf{q}_2$ correspond to the IEC oscillatory periods of $\lambda_1 = 2\pi/|\mathbf{q}_1| = 1.94c$ and $\lambda_2 = 1.52c$, respectively. Although the second period λ_2 is not observed in the calculated IEC, the first one ($\lambda_1 = 1.94c$) agrees well with the first-principles calculation ($\lambda = 1.99c$). Particularly, the model theory predicts a thickness-dependent IEC as $J(R) = -J_0 \sin(|\mathbf{q}_s|R + \phi_s)/R^2$, where J_0 is a thickness-independent item and $\phi = \pi/2$ the phase factor for both $\mathbf{q}_1$ and $\mathbf{q}_2$ [28]. Taking J_0 as an adjusting parameter and utilizing the calculated $\lambda = 2c$, we found that the function ΔE (eV) $= -2.12 \sin(n\pi + \pi/2)/n^2$ describes well the calculated IEC (Fig. 2).

Physically, the nesting vector $\mathbf{q}_s \sim \pi/c$ indicates the Fermi surface is unstable to either the dimerization or the antiferromagnetic ordering of the 1D V chain (i.e., a phonon or a spin-density-wave excitation with $\mathbf{q} = \pi/c$). The latter is not expected in the VO_2 bulk but is possible in the VO_2 spacers of a few nanometers thickness because it had been shown early [29,30] that the 1D long-range magnetic order is unstable to thermal fluctuations so that only nanosized 1D magnetic domains exist. Moreover, as the rutile VO_2 unit cell contains two equivalent V ions, there are two kinds of nearly independent 1D V chains along the c axis. Their spin-density-wave excitations have either the same phase factor or a phase difference of π, corresponding to two distinct magnetic orders in the spacers as (↑↑↓↓ ...) or (↑↓↓↑ ...), respectively. Depending on the configurations of the magnetic DMS layers, they result in the exotic short-range magnetic structures of the multilayers shown in Fig. 3 and consequently in the oscillatory IEC different from the ferromagnetic IEC of the $M1$-phase VO_2 spacers. These significant differences show that, for the VO_2 spacer with n = even, varying the temperature crossing the MIT can reversibly switch the IEC between FM and AFM modes (Fig. 2). The exotic magnetic structures may also indicate that the present DMS multilayers are insensitive to the interface roughness, which has been proven to play a critical role in metallic magnetic multilayers [28,31]. Because the V ions around the interfaces always couple ferromagnetically to the nearby DMS layers, eventually the interface roughness reduces the effective thickness of the VO_2 spacer but may not change the oscillatory period.

To fabricate the temperature-controlled semiconductor GMR devices discussed above, the structural stability of the epitaxial multilayers has to be taken into account. For this reason, we calculate the cleavage energies of the interfaces between the Co-doped TiO_2 and the VO_2 layers based on various optimized multilayer structures (Supplemental Material [21]). It is observed that the saturated value of the interface cleavage energies is about 6.4 J/m^2, stronger than the surface or interface adhesions of most typical element or compound semiconductors such as Si, GaAs, CdTe, etc., whose surface cleavage energies are usually about 1.0 J/m^2 (Supplemental Material [21]). These results indicate that there are rather strong adhesions for both the rutile-rutile and rutile-monoclinic Co-doped TiO_2/VO_2 interfaces despite the different magnetic orders. Moreover, the midinfrared near-field image observations [32] have shown that the MIT of VO_2 starts from nanopuddles of coexisting R- and $M1$-phase VO_2, indicating that both the thickness and the interfaces of the sandwiched VO_2 layer play a less important role in its MIT. Indeed, high-quality VO_2 layers ($\sim$ 10 nm) grown on the TiO_2 (001) single-crystal substrates were found to be fairly stable and were not damaged after many circles of the MIT [33]. Therefore, both theory and experiment evidence the stability of the multilayer devices discussed in this work.

In summary, the IEC of Co-doped TiO_2/VO_2 DMS multilayers is studied theoretically. It is clarified that the electronic-structure instabilities of the VO_2 spacers subject to the phonon and magnon excitations of $\mathbf{q} \sim \pi/c$ lead to

an exotic phenomenon that the IEC can be reversibly switched between FM and AFM modes via the MIT of VO_2. The unique effect paves a way to fabricate a class of temperature-controlled DMS GMR spintronic devices operating at around room temperature.

The work is supported by the National Science Foundation of China (Grants No. 61076089, No. 61227902, No. 11175066, and No. 11074075), the State Key Basic Research Program of China (Grant No. 2013CB922300), and the Ministry of Education of China (SRF for ROCS, SEM).

*ztang@ee.ecnu.edu.cn

[1] M. N. Baibich, J M. Broto, A. Fert, F. N. Van Dau, F. Petroff, P. Etienne, G. Creuzet, A. Friederich, and J. Chazelas, Phys. Rev. Lett. **61**, 2472 (1988).
[2] G. Binasch, P. Grunberg, F. Saurenbach, and W. Zinn, Phys. Rev. B **39**, 4828 (1989).
[3] H. Munekata, H. Ohno, S. von Molnar, A. Segmüller, L. Chang, and L. Esaki, Phys. Rev. Lett. **63**, 1849 (1989).
[4] D. Chiba, N. Akiba, F. Matsukura, Y. Ohno, and H. Ohno, Appl. Phys. Lett. **77**, 1873 (2000).
[5] S. J. Chung, S. J. Chung, S. Lee, I. W. Park, X. Liu, and J. K. Furdyna, J. Appl. Phys. **95**, 7402 (2004).
[6] J.-H. Chung, S. Chung, S. Lee, B. Kirby, J. Borchers, Y. Cho, X. Liu, and J. Furdyna, Phys. Rev. Lett. **101**, 237202 (2008).
[7] J. Leiner, H. Lee, T. Yoo, S. Lee, B. J. Kirby, K. Tivakornsasithorn, X. Liu, J. K. Furdyna, and M. Dobrowolska, Phys. Rev. B **82**, 195205 (2010).
[8] M. J. Wilson, M. Zhu, R. C. Myers, D. D. Awschalom, P. Schiffer, and N. Samarth, Phys. Rev. B **81**, 045319 (2010).
[9] S. Chung, S. Lee, J.-H. Chung, T. Yoo, H. Lee, B. Kirby, X. Liu, and J. K. Furdyna, Phys. Rev. B **82**, 054420 (2010).
[10] T. Jungwirth, W. A. Atkinson, B. H. Lee, and A. H. MacDonald, Phys. Rev. B **59**, 9818 (1999).
[11] T. Jungwirth, J. Mašek, J. Kučera, and A. H. MacDonald, Rev. Mod. Phys. **78**, 809 (2006).
[12] K. Szalowski and T. Balcerzak, Phys. Rev. B **79**, 214430 (2009).
[13] Y. Matsumoto *et al.*, Science **291**, 854 (2001).
[14] W. K. Park, R. J. Ortega-Hertogs, J. S. Moodera, A. Punnoose, and M. S. Seehra, J. Appl. Phys. **91**, 8093 (2002).
[15] V. Eyert, Ann. Phys. (Berlin) **11**, 650 (2002).
[16] D. McWhan, M. Marezio, J. Remeika, and P. Dernier, Phys. Rev. B **10**, 490 (1974).
[17] V. Pardo and W. E. Pickett, Phys. Rev. Lett. **102**, 166803 (2009).
[18] V. Pardo and W. E. Pickett, Phys. Rev. B **81**, 035111 (2010).
[19] M. W. Haverkort *et al.*, Phys. Rev. Lett. **95**, 196404 (2005).
[20] S. Baroni, S. de Gironcoli, A. Dal Corso, and P. Giannozzi, Rev. Mod. Phys. **73**, 515 (2001).
[21] See Supplemental Material at http://link.aps.org/supplemental/10.1103/PhysRevLett.111.107203 for details of the computational method and additional results of the electronic structure calculations.
[22] A. A. Abrikosov, J. Low Temp. Phys. **39**, 217 (1980).
[23] A. Narita and T. Kasuya, J. Magn. Magn. Mater. **43**, 21 (1984); **52**, 373 (1985).
[24] A. Narita, J. Phys. C **19**, 4797 (1986).
[25] V. I. Litvinov and V. K. Dugaev, Phys. Rev. Lett. **86**, 5593 (2001).
[26] M. Luo, Z. Tang, J. Zheng, Z. Q. Zhu, and J. H. Chu, J. Appl. Phys. **108**, 053703 (2010).
[27] M. Luo, Z. Tang, Z. Q. Zhu, and J. H. Chu, J. Appl. Phys. **109**, 123720 (2011).
[28] P. Bruno and C. Chappert, Phys. Rev. Lett. **67**, 1602 (1991); P. Bruno and C. Chappert, Phys. Rev. B **46**, 261 (1992).
[29] L. D. Landau and E. M. Lifshitz, *Statistical Physics* (Pergamon, London, 1959), Vol. 5, p. 482.
[30] N. D. Mermin and H. Wagner, Phys. Rev. Lett. **17**, 1133 (1966).
[31] E. Holmström *et al.*, Proc. Natl. Acad. Sci. U.S.A. **101**, 4742 (2004).
[32] M. M. Qazilbash *et al.*, Science **318**, 1750 (2007).
[33] K. Okazaki, H. Wadati, A. Fujimori, M. Onoda, Y. Muraoka, and Z. Hiroi, Phys. Rev. B **69**, 165104 (2004).